A New Approach for Quantification of 3D Cardiac Wall Motion Tracking Using Active Mesh

S. Kermani, M.H.Moradi, H. Abrishami Moghadam and H. Saneei

***Abstract*—We present a new approach to analysis the deformation of the left ventricle of the heart based on active mesh model that gives a compact representation of a set of points in a 3-D image. It is composed of topology and geometry of the object and associated elastic material properties. The method is image modality independent. The results of evaluation on a four set of image sequence reported in this paper clearly demonstrate the effectiveness of the algorithm.**

I. INTRODUCTION

According to World Health Organization (WHO), at least 20 million people survive heart attacks and strokes every year. Around the world death from heart diseases each year contributes to nearly one-third of global deaths [1]. The Cardiac wall motion is a sensitive indicator of many types of heart disease, such as ischemia. Regional dynamic characterization of the heart wall motion is necessary to isolate the severity and extent of diseases. Quantitative characterization of this motion is essential for the accurate diagnosis and treatment of heart disease. Thus, many studies have been carried out to correlate the dynamic characteristics of the heart with a priori knowledge of various cardiac pathologies. Magnetic resonance imaging (MRI) technology can now provide time varying intrinsic three dimensional images of the heart with excellent contrast, spatial resolution and reasonable temporal resolutions. While, there are rapid ongoing advances in this technological and applications areas, cardiac MRI is still largely a "niche" imaging method that has not been widely adopted as a clinical tool yet [2]. But, more sophisticated quantitative analysis of myocardial dynamics may improve the accuracy in the estimation of myocardial injury.

The specificity of current various cardiac imaging modalities does not allow using alone conventional techniques for motion study like block-matching or optical flow with proper precision [3]. Various models have been introduced previously to study heart wall dynamics. A pseud-3D dimensional active contour model has been used for segmentation volume representation of the heart in a cardiac cycle in [4], [5]. However, these models are not able to do point-wise tracking. In the last few years, many approaches have been proposed to analyze images and extract parameters techniques based on spatio-temporal geometric models have received considerable attention [7]. Deformable models are well suited for this image analysis task [8]. The mathematical foundations of deformable models represent the confluence of geometry, physics, and approximation theory. Geometry serves to represent object shape, physics imposes constraints on how the shape may vary over space and time, and optimal approximation theory provides the formal underpinnings of mechanisms for fitting the models to measured data [9]. The Active mesh among these models permits a large number of degrees of freedom to the object [8]. It has the ability to merge Continuum mechanical constrains and many rules in cardiac wall motions. Alternatively, mesh based algorithms were introduced to segment and track 3D structures in MRI cardiac images [3], [4], [6]. The mesh based tracking methods previously introduced were presented in 2 or Pseudo 3 dimensional space. In our pervious works [10], [11], we presented algorithms for point-wise tracking and analysis of cardiac motion based on 3D active mesh model. But there are several shortcomings in this approach which we try to solve and develop. In this paper these limitations are described and then we propose a new approach to solve and validate them.

II. METHOD

At first, the study on elements which is created by Refined Constrained Delaunay Tetrahedralizations (DCTs) algorithm shows that 40% of elements are between Epicard layer and its surrounding cube and 20% of them are in left ventricular cavity. These elements, according to their nodes are unable to be tracked which impose high Calculation Costs to solve the problem. The cost is extremely raised when the number of elements is increased. For example the calculation time table for an image sequence with a single change in reference frame form ES to ED is as following.

S.Kermani is PhD student of Amirkabir University of Technology, Tehran, Iran (corresponding author to provide phone+98 310 7346 Or+98 311 7922474 ; e-mail *kermani@med.mui.ac.ir*).

M.H.Moradi, is with Faculty of Biomedical Engineering (AUT BME) Amirkabir University of Technology,424 Hafez Ave., Tehran, Iran (E-mail: mhmoradi@aut.ac.ir).

H. Abrishami Moghadam is with BioMedical Engineering Department in Electrical Faculty of K.N.Toosi University of Technology (e-mail moghadam@saba.kntu.ac.ir).

Saneei, Hamid is with the Internal medicince Department, Isfahan University of Medical Sciences, Isfahan, Iran (e-mail:saneei@med.mui.ac.ir).

TABLE I
IN OUR PERVIOUS WORK RUNNING TIME AND MESHING CONFIGURATION FOR TWO REFERENCE FRAME: ES, ED.

	Algorithm Time (sec)	# Mesh ELE	# Mesh Node
Ref: ED	22412	12871	1144
Ref: ES	3447	8353	493
Ratio (%)	650	154	230

The cost is 6.5 times higher for a 2.3 times increase in the number of nodes.

Secondly, we could not use the segmentation results in sparse field estimation. Hence much of the information obtained from segmentation is ignored. Third, in the stage of tracking the points on the surfaces from one frame to the next, these points are not corresponding confidently. While, determining correspondence points there are various confidence measures. Applying these points with identical weight in regularization, results in various errors. Fourthly, rounding the segmentation results in our point-wise tracking is also another source for error. Finally, a possibly better solution would be to incorporate some knowledge of the contraction/relaxation of cardiac muscles during the cardiac cycle. It is possible to manage the deformation of the heart and the imposed mechanical properties of the model by partitioning the systolic and diastolic phase.

A. Improvements desired in motion tracking by the active mesh

By defining and applying a suitable template which covers the left ventricular (LV) muscles environmentally it is possible to reduce the representative elements by 60% (Section B). In order to use the segmentation results completely establishing correspondence of the correspondence points is performed considering the contouring data (Section C). For each pair of correspondence point a confidence measure is determined and used in proposed weighted regularization. Smoothing surface and Rounding noise is eliminated by using Non-shrinkage Gaussian smoothing filter [6]. Usage of initial information of cardiac wall motion phasing is stated in Section D. The procedure of Algorithm comprises the following steps:

1) ROI is selected. 2) ES and ED frame and their interval is selected by user which would be used in partitioning. 3) A suitable frame for making template as the reference frame is selected by the user. 4) After formation of a suitable template for tetrahedralization and meshing it, the refinement of constrained Delauny is used [12]. 5) Cubic spline interpolation is used to convert the voxels to cubic elements for correspondence point procedure. 6) The epi/endocard contour data together with data image set are interpolated and the reference template is partitioned in order to make the dense field estimation possible by enforcing appropriate mechanical properties for each frame which results in a higher performance regularization. Considering that the mechanical specification model of the heart tissue is different in contraction and relaxation [13].

B. Segmentation of the Left Ventricle

The left ventricle on all slices in all frames is segmented interactively by the proposed Algorithm [14]. The method is also based on the concept of deformable models, but extended with an enhanced and fast edge detection scheme that includes temporal information, and anatomical a priori information.

The left ventricular model used in this approach is a time-resolved mesh representation of the LV as an open 'cone', sliced along the cone's long axis with an equal number of points in each slice. The number of points in each slice contour is 80.

C. Creating Template

The mesh generated from the Delaunay triangulation of a general point set is not only a good mesh, but also a unique one and optimized in size and the number of elements. Therefore we use its geometrical representation to make the template. The procedure of creating template comprises the following steps:

1) Creating new contours from segmentation results according to (1).

$$\begin{aligned} X &= X + sign(X_c - X) \quad for\ Surrounding\ EpicardLayer \\ X &= X - sign(X_c - X) \quad for\ Siege EndocardLayer \end{aligned} \tag{1}$$

Where $X = [x_i, y_i, z_i]$ X_c : endo/epicardial centroid

2) Smoothing by Non-shrinkage Gaussian smoothing filter [6]. 3) 3D delauny triangularization for geometrical representation of the LV cavity wall. 4) Creating a general point set to satisfy both non-collinearity and non-cosphericity assumptions. 5) refined constrained Delauny tetrahedralization.

The great advantage of the template is the tangent covering of the whole LV muscle then all edge points are in the template. Thus the tracking becomes easy by decomposing the template into tetrahedral elements.

D. Obtaining initial displacement data, Spares Field

For establishing the correspondence points on epicardial and endocardial contours, we do a weighted correlation-based search only for the points that are on the edge of the 3D epi/endocard in the next frame which have the opportunity to correspond to their previous frame point. The details can be described in the following procedure:

1) Calculate the 3D gradient of current frame image by Soble operator. 2) Determine gradient direction. 3) According to discrete gradient directions, the 3D space around each point is divided into 13 volumic sectors. Therefore, specify major directions and for each direction is defined a 7×7×7 mask. That can be called *direction mask*. 4) For every candidate point: impose its direction mask to a 7×7×7 window centered at the candidate point in the next

frame due to enhancing/enhancement the edge. 5) We correlate a 3×3×3 window centered at the fiducial point in the current frame with the windows from step 4 and 5. The point which gives the maximum cross correlation value is chosen as the corresponding point in the next frame. Then estimate displacement vector measurement B_i from that. 6) The maximum cross correlation value is chosen as confidence measure (C_i).

E. Estimation of Dense Field

Given a set of displacement vector measurements B and confidence measures C from previous stage, let $T=\{V,F\}$ be a tetrahedral defined over the template, where F is a set of tetrahedral and V is a set of its vertices.

F. Formulation of the Kinematic Model

Continuum mechanical models have been used to regularize ill-posed problems in many applications in medical imaging analysis and also for cardiac wall motion tracking. The active elastic model is designed to reduce bias in deformation estimation and to allow the imposition of proper priors on deformation estimation problems that contain information regarding both the expected magnitude and the expected variability of the deformation to be estimated. From finite element theory [10], the strain energy associated with a thin plate is given by (2). ε is the strain energy.

$$\varepsilon=\frac{1}{2}U^T KU \quad U=[..dx_i..|..dy_i..|..dz_i] \quad i=1,2..N \qquad (2)$$

Where U a vector of elementary deformations is, N is the number of vertices and K is the stiffness matrix. The stiffness matrix (similar to the stiffness constant of a spring) may be assembled from elementary stiffness matrices associated with each tetrahedral element [11].

The stiffness matrix is then given by:

$$K=\sum_{e\in f} Ke \quad , \quad K_e=V_e B^T DB \qquad (3)$$

K_e is the element stiffness matrix and V_e is the volume of the element. B is a 6×12 matrix with constant elements defined by the coordination of the vertices of tetrahedral. D is a 6×12 matrix defined by the material properties of the deforming body. The matrix D takes the form [11]:

$$D^{-1}=\begin{bmatrix} \frac{1}{E_p} & \frac{-\nu_p}{E_p} & \frac{-\nu_{fp}}{E_f} & 0 & 0 & 0 \\ \frac{-\nu_p}{E_p} & \frac{1}{E_p} & \frac{-\nu_{fp}}{E_f} & 0 & 0 & 0 \\ \frac{-\nu_{fp}E_f}{E_p} & \frac{-\nu_{fp}E_f}{E_p} & \frac{1}{E_f} & 0 & 0 & 0 \\ 0 & 0 & 0 & \frac{2(1+\nu_p)}{E_p} & 0 & 0 \\ 0 & 0 & 0 & 0 & \frac{1}{G_f} & 0 \\ 0 & 0 & 0 & 0 & 0 & \frac{1}{G_f} \end{bmatrix} \qquad (4)$$

Where E_f is fiber stiffness and E_p is cross fiber stiffness and ν_p,ν_{fp} are the corresponding Poisson's ratios of them and G_f is the shear modulus across fiber $\left(G_f \approx E_f/(2(1+\nu_{fp}))\right)$. The fiber stiffness was set to be 3.5 times greater than cross fiber stiffness. Poisson's ratio was set to 0.4 for both. By choosing E_f =.05, E_p and G_f were calculated. For estimation of the displacement vectors of N Vertex U, we are integrating the data and model terms in

$$\arg\min_{\mathbf{U}} \left\{ \sum_{i=1}^{M} \lambda_i^2 \|d_i-\delta_i\|^2 + \lambda_G \mathbf{U}^T \mathbf{K} \mathbf{U} \right\} \qquad (5)$$

d_i & δ_i are the displacement vector estimation and measurements of point (x_i,y_i,z_i) respectively λ_i,λ_G is *ith* and global regularizing factor. Importance of regularizing term and the *data* term is tuned by $\lambda_i^2=c$. d_i , *ith* estimated displacement vector, is computed by linear interpolation from neighbouring elementary deformation vectors using (6). For a fiducial point P in the tetrahedron (figure1) $\Delta P_k P_l P_m P_n$, the deformation function $d(x,y,z)$ is calculated by (6).

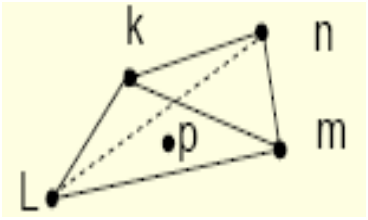

Fig. 1. A fiducial point P in the tetrahedron: linear interpolation(6).

$$d(x,y,z)=g_k(x,y,z)D_k+g_l(x,y,z)D_l+ g_m(x,y,z)D_m+g_n(x,y,z)D_n \qquad (6)$$

where $D_i=(dx_i,dy_i,dz_i)$ theVertex ith

g_i is the ratio volume of tetrahedron fiducial point P and other points except *ith* point to volume $\Delta P_k P_l P_m P_n$.The

above minimization (5) is seen to be equivalent to the minimization (7).

$$\min_U \left\{ \|\lambda AU - \lambda B\|^2 + \lambda_G U^T K U \right\} \text{where} \quad \lambda = [..\lambda_i...] \tag{7}$$

$$A = \begin{pmatrix} Q & 0 & 0 \\ 0 & Q & 0 \\ 0 & 0 & Q \end{pmatrix}_{3m\times 3n}, \quad Q_{ij} = \begin{cases} g_j(x_i, y_i z_i), & j = \{k,l,m,n\} \text{ if} \\ (\hat{x}_i, \hat{y}_i, \hat{z}_i) \in \Delta P_k P_l P_m P_n & \\ 0 \quad , \text{ otherwise} & \end{cases}$$

$$B = [..\delta x_i...|..\delta y_i...|..\delta z_i...]^T \ , \ \delta_i = (\delta x_i, \delta y_i, \delta z_i) \ \ i = 1,...M$$

The solution to (5) is (7), which gives the displacement of all vertices of the mesh. And then by linear interpolation, the displacement of all pixels of the images will be obtained.

III. RESULTS

It is shown that the changes in motion parameters (path length and wall thickening measures) between baseline and post-infarct data are indicative of the myocardial function, and these changes can be used to diagnose the location and extent of myocardial injury, which is validated using post mortem TTC staining technique[6]. The path length of any surface point is the sum of the magnitudes of all displacement vectors of that point over the cardiac cycle, and it measures the overall motion of the point. Wall thickness is defined as the thickness along a radial spike from the endo/ epicardial center.

Wall thickening is defined as (8):

$$\tau' = \frac{\tau_{ED} - \tau_{ES}}{\tau_{ED}} \tag{8}$$

Where τ_{ED} and τ_{ES} are the thickness of the LV wall at ED and ES.

For evaluation of this proposed Algorithm, we used four image sequences, two real (a volunteer and a patient) and two synthetic groups. We reconstructed the deformation field within the myocardium between end-systole and end-diastole for them. Then, two in vivo measures (path length and wall thickening) computed from the algorithm derived trajectories and were compared to those obtained from analytical model of CMRI simulator. Finally, the trajectories which were obtained in two ways (estimated and analytical) were compared.

A. Synthetic Sequence CMRI

We use a computational simulator to generate two set of Gradient Spine Echo Synthetic image sequence. The simulator incorporates a parametric model of Left-ventricular motion due to [15], [16] and applies it to a confocal prolate spherical shell, resembling the shape of the left ventricle. The model can be made to assume a configuration representing one of 60 phases in the cardiac cycle. The inverse motion map analytically, allowing pointwise correspondences to be made between two points at any two times. We simulate a gradient-echo CMRI imaging sequence using intersects model with the plane at arbitrary orientations. In three dimensions, a true motion is output so that motion estimation algorithms can be compared against the truth. We contaminated these images with normally distributed random noise in the determined SNR. Another imaging sequence is generated the same but mechanical parameters are changed in the lateral basal region as a simulation of akinetic region area.

The specification of *confocal prolate spherical shell model* is:

$$\begin{aligned} x &= \delta \sinh\lambda \sin\eta \cos\varphi \\ y &= \delta \sinh\lambda \sin\eta \sin\varphi \\ z &= \delta \cosh\lambda \cos\eta \\ &where \quad \delta = 5, \ \lambda = 0.4{:}0.6 \\ &0 \le \eta \le 120 \quad 0 \le \varphi \le 360 \end{aligned} \tag{9}$$

According to the LV wall volume is constant and almost equal 100 cm^3 and the LV cavity volume is changed from 60 to 120 cm^3 during a cardiac cycle. The image sequence is $64\times64\times60\times64$ and its resolution is 1.1mm in the 3D. The spatial and temporal dimension is decreased to $64\times64\times15\times12$, like the standard CMRI sequence. Table 2 is the comparison between dense motion fields provided by Algorithm with its Analytical value. You see MSE value versus SNR value. It seems that the proposed approach is robust. Despite of the refined meshing object, the running time of Algorithm is 1/3 of our previous Algorithm [11] due to elimination of redundancy nodes and elements outside the cardiac wall.

In Figure 2, Bulls eye of normalized path-length estimated motion field (right) and the Analytical values (Left) of two synthetic image sequences in entire cardiac cycles is shown. The akinetic region completely detected and there are significant differences between the values of the base and akinetic area (yellow in basal ant. lateral and basal ant.) .The extraction of motion field is also robust to noise. Figure 3 is the MSE of motion field vs. frame where the mean value of all frames is $0.85\% \pm 0.4$ for zero SNR.

TABLE II
ESTIMATED DENSE MOTION FIELDS COMPARE WITH THEIR ANALYTICAL FIELDS.

SNR	0	5	10	20
Mean Err (%)	0.845	0.816	0.77	0.78
Running Time (s)	878	815	810	811

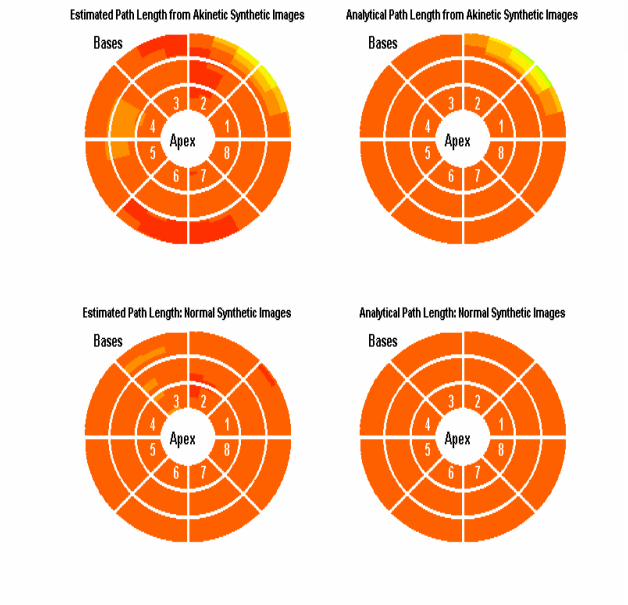

Fig. 2. Comparison between normal (down) and abnormal (up) Bulls eye of normalized Path Length. (1 through 8 are lat, ant ,sept and inf regions respectively.)

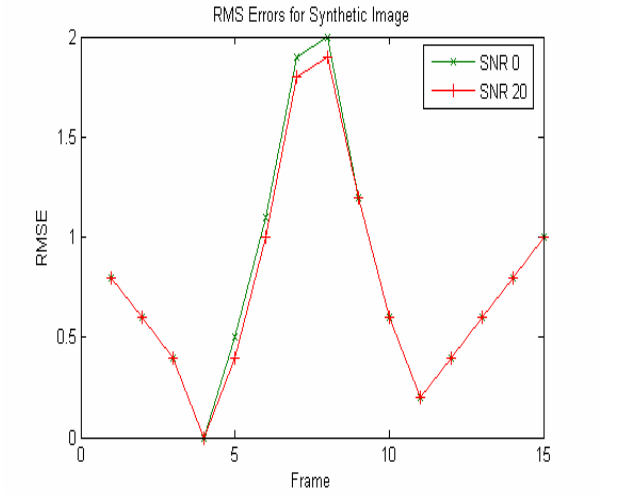

Fig. 3. RMS Errors for Synthetic Image Sequences in two SNR levels.

B. Real Sequence

The result of evaluation on two set of Gradient-Echo images is given in this section. MR imaging was performed on a Symphony Siemens 1.5 Tesla scanner. Short-axis images through the left ventricle were obtained with the turboGSE cine technique using the following parameters: TR = 43.44ms, TE = 1.59 ms, FA = 53°, SL = 5mm, the protocol Name is tf2d20_12Slices_ shph_12bh. With this protocol, Short breath-hold scans and multi slice applications in one breath-hold are possible. The contrast is a function of $\frac{T1}{T2^*}$ and independent of TR. The two set data contain 16/21 frames per cardiac cycle, each frame containing 10/ slices with an in-plane resolution of 0.73/0.97mm×0.73/0.97mm. The data refers to a volunteer/patient. In Figure 4, the MRI cardiac data of a volunteer is shown. In these images, the region containing the left ventricle is selected hence the size of the image matrix is reduced to 128×128. In Figure 5, the result of template of the left ventricle wall for the ED phase of cardiac cycle is shown. In Figure 6, the result of tracking the left ventricular wall by active mesh algorithm is shown. The results show that the algorithm can track the cardiac motion in all 3 dimensions with acceptable accuracy. In Figure 7, the result of trajectory of a set of points is seen in 2D. The result of normalized and compensated path-length and wall thickening in 8 regions for patient's data set shows a significant reduction in abnormal regions. These results are matched with those obtained from the patient's thallium scan modalities.

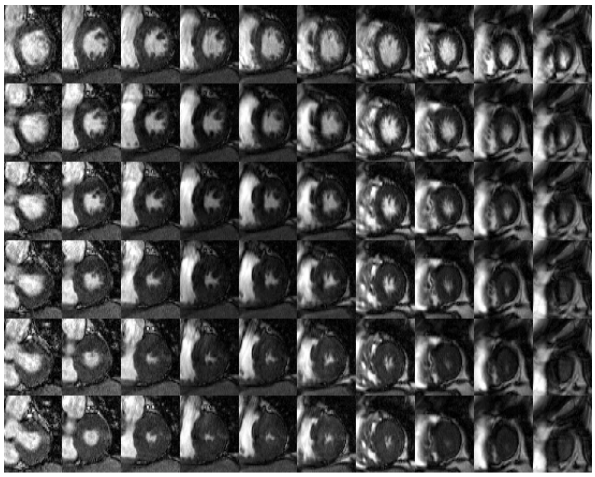

Fig. 4. The MRI Cardiac Data of a Volunteer.

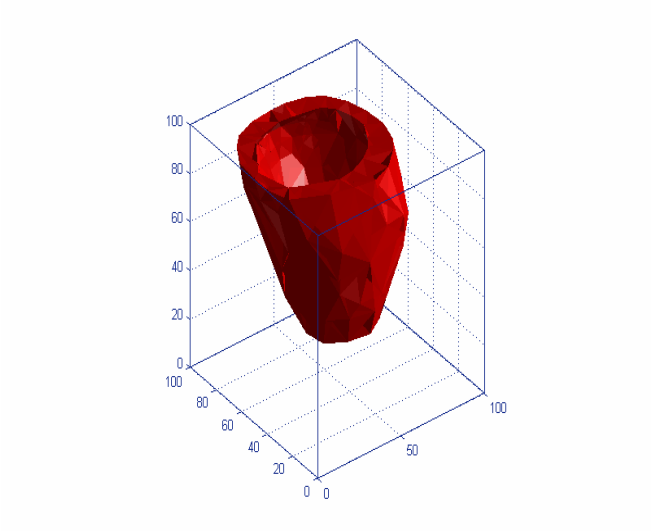

Fig. 5. The Template of the Left Ventricle Wall for the ED Phase of Cardiac Cycle.

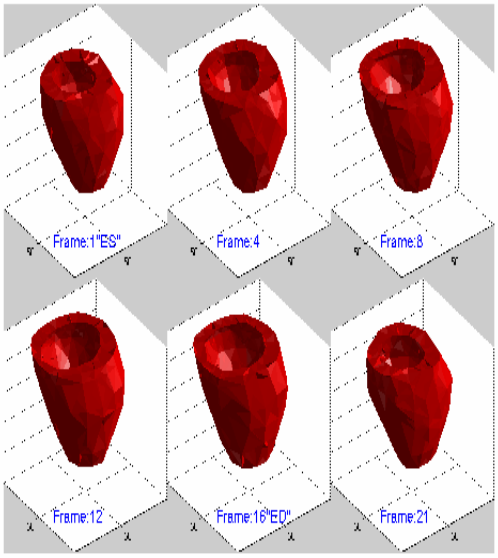

Fig. 6. Result of the Left Ventricular Wall Tracking by our Algorithm.

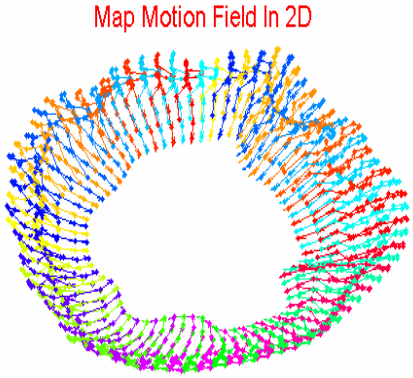

Fig. 7. The Trajectory of a Set of Myocardial Points mapped in 2D.

IV. Discussion and Conclusion

In this paper we have presented a new method for tracking the motion of the myocardium in the LV using active Mesh. The active mesh model is a generalization of the original elastic model which penalizes deformations away from a preset value as opposed to simply all deformations. We reconstructed the deformation field within the myocardium for one volunteer and one patient and two synthetic data sets. Experiments were performed on those clearly demonstrate the effectiveness of our algorithm for extracting motion parameters. The tracking algorithm is very fast and robust. it may be used for extraction and analysis of the full four-dimensional deformation field within the myocardium of the LV. To do this we make use of short-axis (SA) images of the LV.

Further and future research involves assessment and improvements of the tracking software for larger data sets are foreseen. Some works are in progress to integrate cardiac muscle nonlinearity into our model. In addition, we plan to combine the present correlation-based search method with shape-based tracking method which seems to be better choice for perpendicular and tangential motion estimation.

V. Acknowledgements

Isfahan MRI Center, for kind cooperation in cardiac image acquisition.

References

[1] World Health Organization (WHO), *cardiovascular disease: prevention and control*.

[2] Axel, L. 2004. *"CARDIAC MRI ".Biomedical Imaging: Macro to Nano*, IEEE International Symposium on 15-18 April P.1212 - 1214 Vol. 2.

[3] Lautissier J., Legrand L., Lalande A., Walker P., Brunotte F., 2003*." Object tracking in medical imaging using a 2D active mesh system"* , Proceedings of the 2 5 ~ Annual Intemational Conference of the IEEE BMBS Cancun, Mexico September P 17-21.

[4] Paragios N., 2003. *A level set approach for shape-driven segmentation and tracking of the left ventricle*, IEEE Trans. Med. Imag. Vol.22 P 773–776.

[5] Abrishami Moghaddam H., Lerallut J.F., 1998. *Volume Visualization of the Heart Using MRI 4D Cardiac Images*. Journal of computing and information technology, Vol. 6, P 215–228.

[6] Shi P., Sinusas A.J., Constable R.T., Ritman E., and Duncan J.S., 2000. *Point-Tracked Quantitative Analysis of Left Ventricular Surface Motion from 3-D Image Sequences*, IEEE Trans. Med. Image, Vol. 19, P 36–50.

[7] Frangi A, Niessen W, Viergever M., 2001. Three-*dimensional modeling for functional analysis of cardiac images: A review*. IEEE Trans. on Medical Imaging 20 ; p 2-25.

[8] Montagnat J, Delingette H., Ayache N., 2001. *"A Review of Deformable Surfaces: Topology, Geometry and Deformation"*, INRIA, INSA Lab Report.

[9] McInerney Tim and Terzopoulos Demetri, 1996.*,"Deformable Models in Medical Image Analysis: A Survey Medical Image Analysis"*, 1(2):91–108.

[10] Mosayebi P., Abrishami Moghaddam H., and Giti M., 2006. *A Fully 3D Active Mesh Model for motion Tracking in Cardiac MRI"* MICCAI workshop, vol. 1, P 131-138.

[11] Jamali Dinani F.,Mosayebi P.,Abrishami Moghaddam H., Giti M and Kermani S., 2007.*"FIMH 2007* P. 12-21.

[12] Si H., 2006.*"On Refinement of Constrained Delaunay Tetrahedralizations"*. In Proceedings of the 15th International Meshing Roundtable.

[13] Hu Z., Metaxas D., Axel L. ,2005. *"Computational Modeling and Simulation of Heart Ventricular Mechanics with Tagged MRI"* ACM.

[14] Heiberg E., Wigström L., Carlsson M., Bolger A.F., Karlsson M.,2005. *Time Resolved Three-dimensional Segmentation of the Left Ventricle*, In proceedings of IEEE Computers In. Arts, W.

[15] Hunter C., Douglas A., Muijtjens A. M. M., and Reneman R. S., 1992. *"Description of the deformation of the left ventricle by a kinematic model*," J. Biomech., vol. 25, no. 10, p. 1119–1127.

[16] Waks E., Prince J. L., and Douglas A., 1996. *"Cardiac motion simulator for tagged MRI*," in Mathematical Methods in Biomedical Imaging Analysis, p. 182–191.